Deterministic Lateral Displacement (DLD): Finite element modeling and experimental validation for particle trajectory and separation

E. Pariset[*,**], J. Berthier [*,**], F. Revol-Cavalier[*,**], C. Pudda[*,**], D. Gosselin[*,**], F. Navarro[*,**], B. Icard[*,**], V. Agache[*,**]

[*] CEA, LETI, MINATEC Campus, F-38054 Grenoble, France
[**] Univ. Grenoble Alpes, F-38000 Grenoble, France

ABSTRACT

In biotechnology, deterministic lateral displacement (DLD) is used to separate label-free particles — such as cells, bacteria and exosomes — according to their size. The separation phenomenon is based on steric effects around an array of shaped micro-pillars: particles larger than a critical size are laterally displaced by the pillars whereas smaller particles follow a global straight path. Models have been proposed in the literature to predict the critical sizes according to the geometry of the DLD arrays. However, these models are semi-empirical and do not cover all the possible pillar shapes and orientations. Here we present a finite element model to find the best separation geometries for different-shaped micro-pillars, using COMSOL finite element particle tracing module. Calculation results are compared to the literature and confirmed by experimental results with calibrated polystyrene particles. Therefore, the presented model allows to choose the optimal DLD design according to the desired separation size.

Keywords: deterministic lateral displacement, finite element model, particles separation, design optimization

1 INTRODUCTION

Deterministic lateral displacement (DLD) is a microfluidic particle-separation technique that makes use of successive bifurcations of the laminar flow around an array of regularly arranged pillars. This technique enables to separate nanometer to micrometer-sized particles around a critical diameter called D_c, that is determined by several geometrical characteristics of the posts array, such as the pillars shape, orientation, inter-spacing and slant angle.

The separation principle implemented in DLD systems was first described in 2004 by Huang et al. [1]. The DLD array contains many rows of pillars that are horizontally shifted when compared to the direction of the fluid flow. Therefore, the fluid emerging between two pillars is separated into several flow tubes when flowing around the next pillar. The number of streamlines and their width are related to the slant angle and the inter-spacing gap between two adjacent pillars. When particles are injected, their trajectory in the DLD array is determined by their radius when compared to the width of the first flow tube that is not deviated by the pillar. When the particle's radius is smaller than the width of this flow tube, the particle follows a global straight "zigzag" path, while larger particles are "displaced" by the pillars because of steric effects. The critical diameter (D_c) defines the transient size between both trajectories.

In 2006, Inglis et al. [2] proposed a model to predict the value of D_c for circular posts and an infinite DLD channel, with the assumption of a parabolic flow profile between adjacent posts. By integrating the flow profile along the width of the first flow tube, the ratio of the critical diameter D_c over the inter-spacing gap G was obtained, if θ is the slant angle, and ε = tan(θ):

$$\frac{D_c}{G} = \mathrm{Real}\left(1 + 2w + \frac{1}{2w}\right) \quad , where$$
$$w = \left(\frac{1}{8} - \frac{\varepsilon}{4} + \sqrt{\frac{\varepsilon}{16}(\varepsilon - 1)}\right)^{1/3} \left(-\frac{1}{2} - \frac{i\sqrt{3}}{2}\right) \tag{1}$$

By matching experimental data obtained with rigid particles and circular pillars, Davis [3] was able to propose a prediction of D_c with good agreement with Inglis' model:

$$D_c = 1.4 G \varepsilon^{0.48} \tag{2}$$

Triangular pillars were considered by Loutherback et al. [4] to improve separation performances. The Inglis model was adapted to take into account the asymmetric flow profile presented between triangular posts and good agreement with experimental results was obtained.

Recently, Davis' model was refined to generalize to several pillar shapes from numerical results. From a lattice Boltzmann method, Wei et al. [5] modelled the separation of hard spherical particles in DLD networks with five different post shapes. A new factor called ratio of sub-channel widths η was introduced in the Davis formula to take the pillar shape into account in the prediction of D_c.

$$D_c = 1.4 \alpha G \varepsilon^{0.48} \quad \text{and} \quad \alpha = \frac{1}{N} k(\eta) + b(\eta) \text{, where}$$
$$N = 1/\varepsilon \tag{3}$$
$$k = -2.045 + 4.021\eta - 1.281\eta^2$$
$$b = 0.325 + 0.123\eta + 0.059\eta^2$$

Zhang et al. [6] injected two geometric factors α and β in the Davis formulation in order to predict the effect of four different post shapes on the critical diameter from dissipative particle dynamics modelling.

$$D_c = \alpha G \varepsilon^{\beta} \quad (4)$$

Unlike in the Wei model, it was found that the α parameter was not affected by the pillar shape, while the β parameter was different for circular, triangular, diamond and square pillars.

In this paper, a new model is presented to predict the critical diameter in DLD arrays of different shaped and oriented micro-pillars, using COMSOL finite element particle tracing module. The calculation is compared to the models that were introduced above as well as to experimental data with rigid spherical polystyrene particles.

2 FINITE ELEMENT MODEL

A commonly made assumption is that the particles do not modify the flow pattern. In other words, the particle trajectory is weakly coupled to the hydrodynamics. Note that this assumption may fail with highly concentrated samples, like whole blood. In the COMSOL approach, the hydrodynamics of the carrier fluid is first computed. The particle trajectory computation requires to solve the Newton equation for each particle, taking into account inertia, gravity and drag force. However, the use of the COMSOL module "Particle Tracing" needs refinements to take into account the wall-exclusion. A particle position should not be only determined by its barycenter, but also by its envelope. We have set up on any solid boundary — in our case the pillars and channel walls — a rebound condition based on the distance from the particle barycenter to the wall, so that the particle envelope does not intersect the wall surface.

2.1. The notion of distance to the walls

The distance from a point of the computational domain to the boundary is given by the Eikonal equation:

$$\left|\nabla d(x)\right| = 1 \quad (5)$$

The Eikonal equation requires that the distance to the walls function d(x) is well-behaved — in the present case differentiable — at the walls. This restriction stems from the remark that the distance function on the boundary is:

$$\nabla d(x|_{\partial\Omega}) = n(x) \quad (6)$$

where n is the inward normal to the boundary Ω. The normal unit vector on pillars with sharp edge is not defined, and this induces a singularity. The introduction of rounded edges solves this problem.

2.2. The steric effect

Once the wall-distance map is calculated, the steric effect of the particles can be implemented. Indeed, the particle contacts the wall when d(x) is equal to the particle radius and its velocity is directed towards the wall. Upon contact, a rebound condition is set up:

$$\vec{n}.\vec{V}_{p,rebound} = -\vec{n}.\vec{V}_p \text{ and } \vec{t}.\vec{V}_{p,rebound} = \vec{t}.\vec{V}_p \quad (7)$$

Figure 1 shows two populations of particles of different sizes (diameters 7 and 7.2 µm), transported by a carrier fluid, moving around circular pillars (diameter 15 µm). The calculation of the particle-wall distance (Fig. 1b) is essential to model the separation effect around the critical diameter.

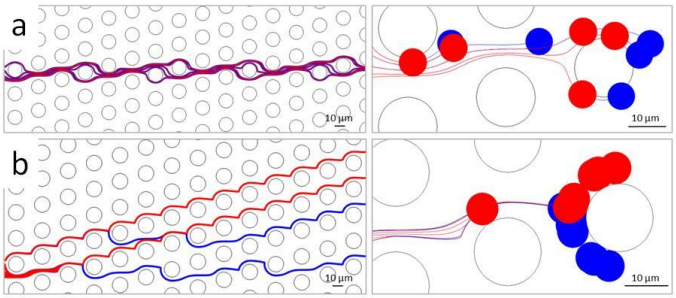

Figure 1: Modelisation of the DLD separation without (a) and with (b) the wall distance physics

3 NUMERICAL RESULTS

From this numerical model, we were able to determine the influence of the pillar shape and orientation on the critical diameter and to compare our results to the literature. Rigid spherical particles were injected in several 2D DLD arrays. First, our model for circular pillars has been validated by a comparison with the results of Davis [3] and Inglis et al. [2].

3.1 Validation for circular pillars

For each DLD array geometry, the critical diameter was determined from the mode of displacement of different sized particles. Three types of trajectory were observed in the simulations according to the particle size: the zigzag and displacement modes, as well as a "mixing mode" with alternation of zigzag and displacement modes for particle sizes close to the critical diameter [7]. The numerical critical diameter was defined as the smallest particle diameter for which a displacement mode was observed.

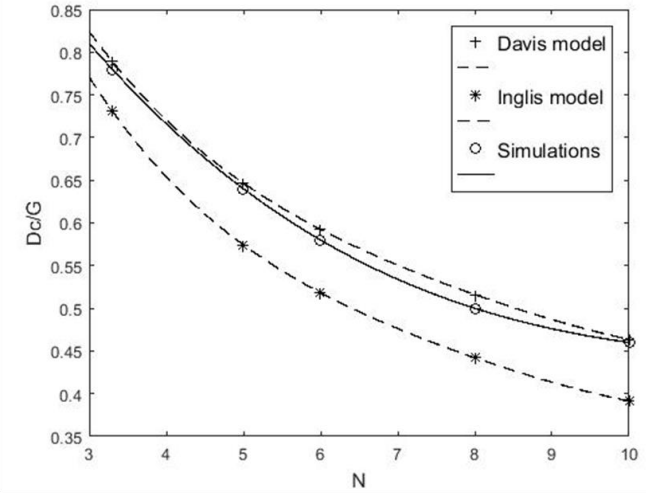

Figure 2: Comparison of D_c/G between the Davis and Inglis models and the numerical results with $N=1/\varepsilon$

Figure 2 shows good agreement of our numerical results with Davis' model., while Inglis' model is shifted towards smaller critical diameters. This suggests that the assumption of a parabolic flow profile between adjacent posts does not match exactly experimental and numerical results. Refinements should be considered to take into account the anisotropy induced by the slant of the pillars array.

3.2 Effect of shape and orientation of pillars

The number of geometrical parameters that describe the pillars are numerous: shape, orientation, spacing and period number. Here, we investigate numerically the influence of the pillars shape and orientation on 15µm-width posts, with an inter-pillars gap of 10µm. Five geometries were considered: circles, hexagons, octagons and triangles with two orientations for hexagons and triangles.

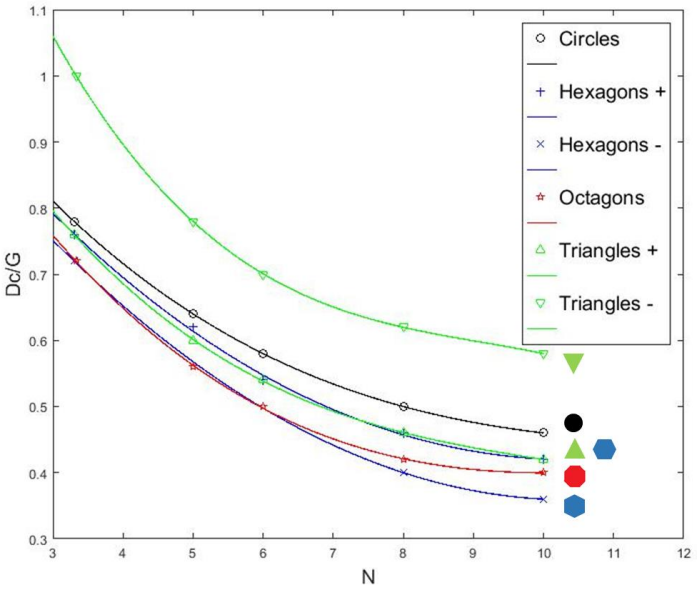

Figure 3: Diagram of the critical diameters for pillars with different shapes and orientations

Figure 3 shows that both the shape and the orientation of pillars influence the critical diameter.

The effect of the pillar orientation is represented in Figure 4 with a flow going from the left to the right side. When compared to a vertical post edge (Fig. 4b), the critical diameter decreases with a positive slope of the post edge (Fig. 4a), as the streamlines are directed upwards, and it increases with a negative slope (Fig. 4c), as the streamlines are directed downwards.

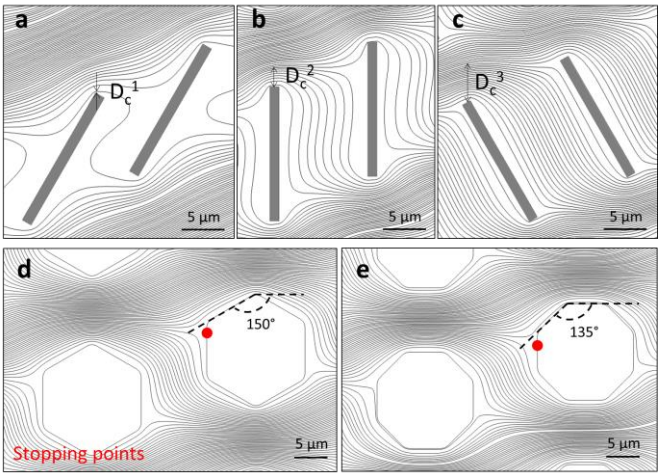

Figure 4: Comparison of the streamlines distribution around the same rectangular pillars with three different orientations (a-c), hexagonal (d) and octagonal pillars, with N=3.3

It is verified in Figure 3 that D_c is larger for negative-slope triangles (triangles -) than for positive-slope triangles (triangles +). The other pillar geometries have two possible orientations as they have a top-down symmetry. However, even with the smallest value of N that is considered, only the top-half section of the pillars is approached by the streamlines flowing above the previous pillar (Fig. 4d and 4e). Therefore, the hexagonal and octagonal pillars have similar D_c values as the positive-slope triangles. Since the triangles + and hexagons + pillars have the same slope for the left edge (120°-slope), they have the same D_c diagram. For small N values, the critical streamlines approach a vertical edge for both hexagons - and octagons since the stopping point is located on this edge (in red in Fig 4.d and e), which explains that both D_c diagrams are the same. When N increases, the influence of the edge slope appears and D_c becomes larger for octagons (135°-slope) when compared to hexagons – (150°-slope).

The model adapted from Davis [5][6] was applied to our simulation results in order to find the α and β parameters in the equation (4). Table 1 shows the obtained parameters:

Pillar Shape	Circle	Hex. +	Hex. -	Oct.	Tri. +	Tri. -
α	1.4	1.4	1.4	1.4	1.4	1.1
β	0.48	0.54	0.60	0.53	0.54	0.49

Table 1: Values of the geometrical parameters α and β

As suggested by Zhang et al. [6], we confirm that the α parameter is the same as in the Davis formula for all the geometries, except for inverted triangles. Therefore, the α parameter seems to represent the orientation of the post edge that is encountered by the particles flow. The β parameter is a characteristic of each pillar shape with a decrease in β when the slope of the post edge increases.

4 EXPERIMENTAL RESULTS

Experimental validation was performed on circular and triangular pillars with G=20µm and N=50. Figure 5 shows the trajectory of rigid spherical polystyrene beads with fluorescent labelling (Thermo Fisher Scientific, G0300, G0500 and CDG1000). When recording the images (Olympus XM10 CCD camera), the exposure time was set large enough so that the particle trajectory appears as a continuous white line. Figure 5 confirms that D_c is larger for circular pillars than triangular pillars for identical inter-pillars gap and slant angle. Indeed, 5µm-beads have a zigzag trajectory when flowing in the circles array but they display a displacement mode in the triangles array. It is demonstrated here that Dc is comprised between 5µm and 10µm with circles, while it is comprised between 3µm and 5µm with triangles.

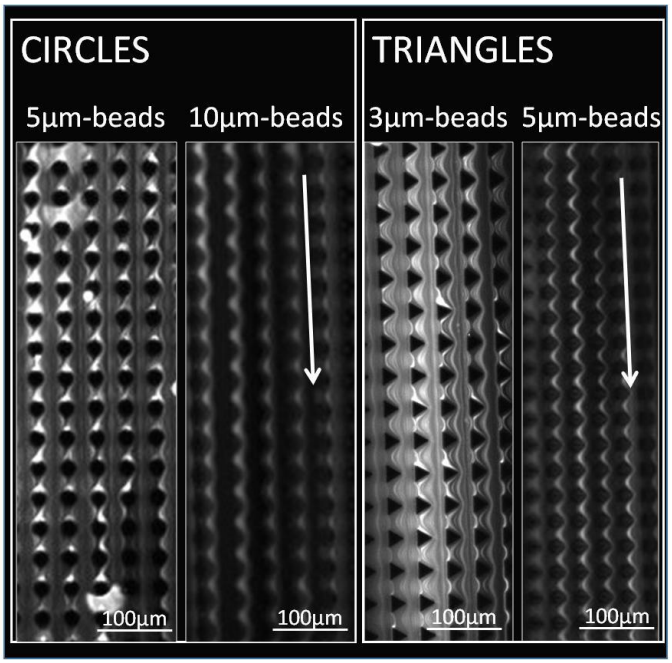

Figure 5: Trajectory of different sized polystyrene particles in DLD arrays with identical geometric parameters except the pillar shape (circles or triangles). The orientation of the pillars is given by the arrows.

5 CONCLUSION

In this work, a finite element model coupled to a particle trajectory model has been implemented using the COMSOL numerical program. The approach enables to study the influence of pillars shape and orientation on the separation diameter in DLD arrays. The results for circular pillars are in agreement with results from the literature. For non-circular pillars, it has been demonstrated that the orientation of the pillar edge influences the critical diameter. The Davis model was adapted to match our numerical results. While Wei et al. [5] proposed a single geometrical parameter for each pillar shape, independently of the orientation of the pillar, we have considered both the shape and the orientation of the posts at the same time. In order to be even closer to experimental results, two additional factors should be taken into account: the streamline anisotropy linked to strongly assymmetric pillars [8] and the boundary conditions at the channel walls.

REFERENCES

[1] L. R. Huang, E. C. Cox, R. H. Austin, and J. C. Sturm, "Continuous particle separation through deterministic lateral displacement," *Science*, vol. 304, no. 5673, pp. 987–990, May 2004.

[2] D. W. Inglis, J. A. Davis, R. H. Austin, and J. C. Sturm, "Critical particle size for fractionation by deterministic lateral displacement," *Lab. Chip*, vol. 6, no. 5, pp. 655–658, May 2006.

[3] John Alan Davis, "Microfluidic Separation of Blood Components through Deterministic Lateral Displacement," *Diss. Present. Fac. Princet. Univ. Candidacy Degree Dr. Philos.*, Sep. 2008.

[4] K. Loutherback, K. S. Chou, J. Newman, J. Puchalla, R. H. Austin, and J. C. Sturm, "Improved performance of deterministic lateral displacement arrays with triangular posts," *Microfluid. Nanofluidics*, vol. 9, no. 6, pp. 1143–1149, May 2010.

[5] J. Wei *et al.*, "Numerical Study of Pillar Shapes in Deterministic Lateral Displacement Microfluidic Arrays for Spherical Particle Separation," *IEEE Trans. Nanobioscience*, vol. 14, no. 6, pp. 660–667, Sep. 2015.

[6] Z. Zhang, E. Henry, G. Gompper, and D. A. Fedosov, "Behavior of rigid and deformable particles in deterministic lateral displacement devices with different post shapes," *J. Chem. Phys.*, vol. 143, no. 24, p. 243145, Dec. 2015.

[7] T. Kulrattanarak *et al.*, "Mixed motion in deterministic ratchets due to anisotropic permeability," *J. Colloid Interface Sci.*, vol. 354, no. 1, pp. 7–14, Feb. 2011.

[8] R. Vernekar, T. Krüger, K. Loutherback, K. Morton, and D. Inglis, "Anisotropic permeability in deterministic lateral displacement arrays," *Phys. Flu Dyn*, Oct. 2016.